Excerpt from the Proceedings of the 2011 COMSOL Conference in Boston

Non-Equilibrium Quantum Well Populations and Optical Characteristics of III-Nitride Lasers and Light-Emitting Diodes

Mikhail V. Kisin*, Hussein S. El-Ghoroury
Ostendo Technologies, Inc.
*Corresponding author: 6185 Paseo del Norte, Ste. 200, Carlsbad, CA 92011, mikhail@ostendo.com

Abstract: COMSOL-based Ostendo's Optoelectronic Device Modeling Software (ODMS) has been updated to include effects of non-equilibrium QW populations in semiconductor light-emitting and laser diodes. III-nitride light emitters with different levels of polarity have been compared as an illustrative example of ODMS performance. Modeling proved that high intra-QW recombination rates in III-nitride light emitters make the QW populations strongly non-equilibrium and vulnerable to inhomogeneous injection in multiple-QW devices. QW populations are further affected by disparate electron and hole transport across the active region.

Keywords: Optoelectronics, lasers, light emitting diodes, quantum wells, carrier injection.

1. Introduction

III-nitride light emitting structures provide technological basis for development of solid-state lighting devices, high definition optical data storage and a number of other applications. COMSOL-based Ostendo's Optoelectronic Device Modeling Software (ODMS) [1] has been extensively used in the design and performance analysis of III-nitride lasers and light emitting diodes [2,3] and III-V mid-infrared devices [4].

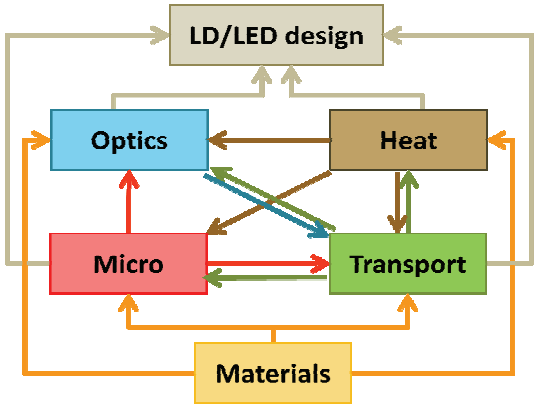

Figure 1. Flowchart of ODMS software. No specific COMSOL modules have been employed by ODMS.

The software was recently updated to include hot-carrier effects into ODMS "Transport" module [5] which allowed more accurate simulation of carrier injection and leakage processes in electrically inhomogeneous multi-QW active regions [6]. In this paper, we report on next "Micro"- and "Transport"-module updates which include into modeling the rate equations for electron and hole populations of active QWs. We show that in deep III-nitride QWs high rates of radiative and nonradiative recombination make the QW populations highly non-equilibrium. Asymmetrical injection of electrons and holes further impairs the QW population balance. In multiple-QW active regions, residual QW charges strongly increase the inhomogeneity of QW injection.

2. Use of COMSOL Multiphysics

ODMS pays special attention to detailed microscopic modeling of quantum carrier confinement and radiative characteristics of active QWs. Valence subband spectrum of confined holes is calculated in "Micro" module using the Rashba-Sheka-Pikus 6x6 matrix Hamiltonian for strained wurtzite semiconductors in arbitrary crystallographic configuration [2]. The resulting multi-band equation system for QW eigenstates is solved by COMSOL eigenvalue solver self-consistently with Poisson's equation taking into account effects of intra-QW polarization screening and thermal carrier redistribution between the QW subbands and contiguous extended 3D carrier states. QW radiative characteristics have been calculated by linked MATLAB programs performing *k*-space and spectral integrations of interband optical transitions for each pair of QW subbands. This automatically includes into our simulations the effect of radiative time saturation due to electron and hole phase-space filling at high QW injection levels.

Current update includes into "Micro" module tasks the solution of a rate equation system for non-equilibrium electron and hole populations of

the modeled QW. The system is solved by stationary nonlinear COMSOL solver and connects the confined electron and hole QW populations to the mobile populations of extended bulk-like states of the QW layer. At this stage of model development, QW carrier capture and non-radiative recombination processes are treated phenomenologically.

Rate equation solutions are linked to the "Transport" module and used in the injection modeling to tie the non-equilibrium confined QW populations to the injection levels in mobile carrier subsystems. In transport simulation, ODMS uses quasi-Fermi levels of mobile electrons and holes as independent variables; non-equilibrium QW populations strongly depend on both arguments and are determined self-consistently together with the resulting intra-QW recombination rates which then enter the system of continuity equations for electron and hole currents. Continuity equations for mobile carriers are solved self-consistently with Poisson's equation for residual charges by using COMSOL stationary nonlinear solver.

3. Simulation Example

To demonstrate ODMS capabilities, we performed comparative simulation of three III-nitride light-emitting diode structures grown in different crystallographic orientation, (0001), (11-22), and (11-20), and characterized by different level of microscopic polarization being, correspondingly, polar, semipolar, and nonpolar. Widths and compositions of active QWs have been chosen to provide for the same emission wavelength at high injection level. QW widths

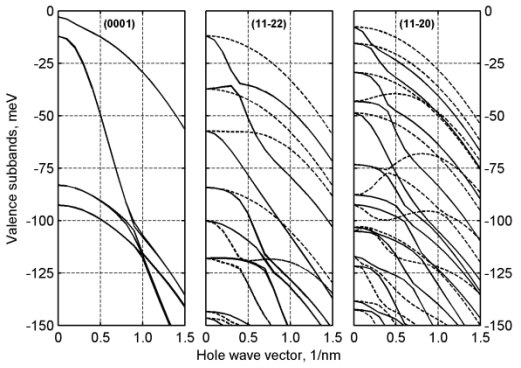

Figure 1. Valence subband structure in polar (0001), semipolar (11-22) and nonpolar (11-20) QWs.

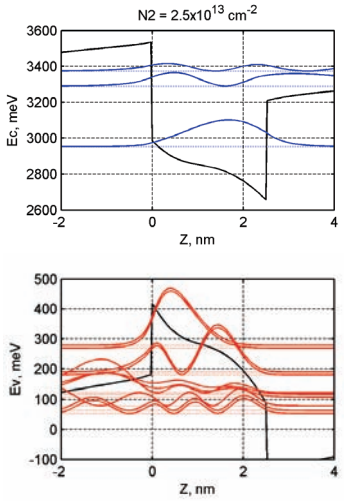

Figure 2. Zone-centered electron and hole eigenstates in polar (0001) QW at high injection level.

of 2.5nm, 4.0 nm and 8.0 nm have been adopted to compensate for lower Indium intake in low-polarity QWs.

Figure 1 compares the structure of valence subbands in all three modeled QWs. Figure 2 illustrates the spatial distribution of confined electron and hole states in the polar QW. Strain-induce splitting of upper valence subbands in semipolar QW readily seen in Figure 1 provides for strong TE-gain enhancement in stimulated emission spectra presented in Figure 3. Figure 4 shows radiative coefficient of polar QW presented as 2D-function of electron and hole equilibrium QW populations. Noticeable increase of radiative output at high QW injection levels represents the beneficial effect of intra-QW screening on electron-hole overlap.

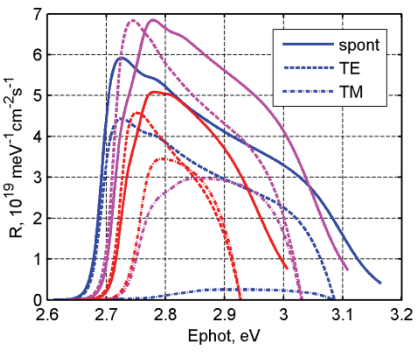

Figure 3. Spontaneous and stimulated emission rates in polar, semipolar and nonpolar QWs. N=3x10^{13}/cm^2.

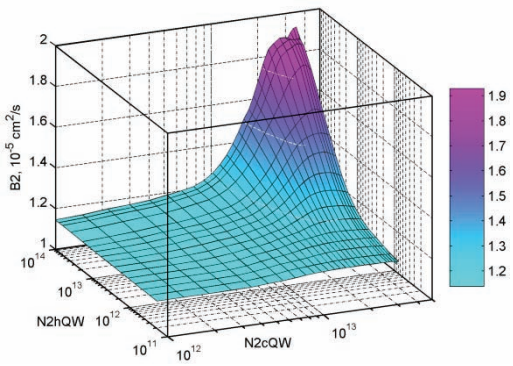

Figure 4. Radiative recombination coefficient in polar QW vs. electron and hole equilibrium injection levels.

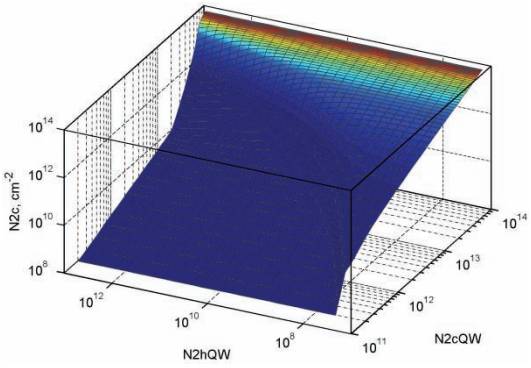

Figure 5. Nonequilibrium electron population in nonpolar QW vs. equilibrium carrier injection levels.

Figure 5 illustrates the extent of the non-equilibrium effects in QW population process. It is readily seen that the effective electron concentration in the QW strongly declines with hole injection. The top of the 2D surface plot at the highest levels of electron injection of about $4x10^{13}/cm^2$ represents the finite capacity of the electronic QW.

In polar III-nitride diodes, polarization charges at the structure interfaces induce high potential barriers for carrier transport. Strong electrical inhomogeneity of the polar active region aggravates the carrier leakage and provides the conditions for the active region ballistic overshoot by hot electrons. Figure 6 compares conduction band profiles (upper panel) and injected current component distributions (lower panel) in polar and semipolar 3-QW diode structures. Notably, even in nonpolar structures, QW injection conditions are affected by highly non-equilibrium character of active QW populations and large residual QW charges. Figure 7 provides necessary details. Left panel presents a cross-section of 2D plot in Figure 5: the set of curves shows the non-equilibrium electron population in polar QW as a function of the equilibrium level of QW hole injection; the level of electron injection serves as a curve set parameter. The curve crowding at the highest levels of electron injection corresponds to the electron QW overflow. The hole QW with higher DOS allows much higher population. It is readily seen that at higher level of electron injection (upper curves of the set), the higher hole injection is required for non-equilibrium effects to step in. For all realistic carrier injection levels, the actual non-equilibrium electron QW popula-

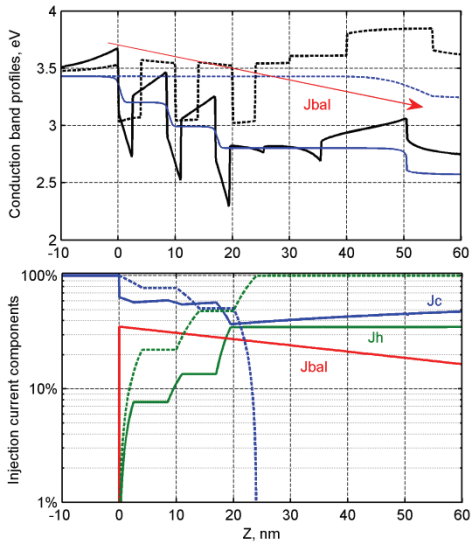

Figure 6. Conduction band and current component profiles in polar (solid lines) and semipolar (dashed lines) 3-QW diode structures at 1 kA/cm^2 injection.

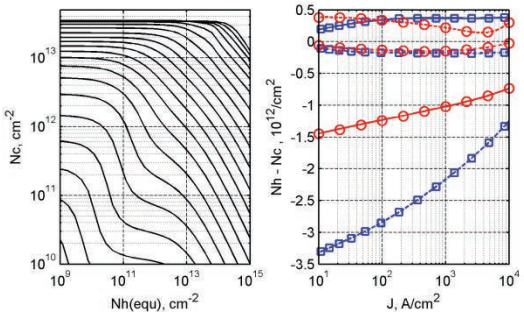

Figure 7. Nonequilibrium electron population in nonpolar QW and residual QW charges in 3-QW polar and nonpolar diodes. Solid: N-side QWs, dashed: p-side QWs, dash-dotted: middle QWs (neutral).

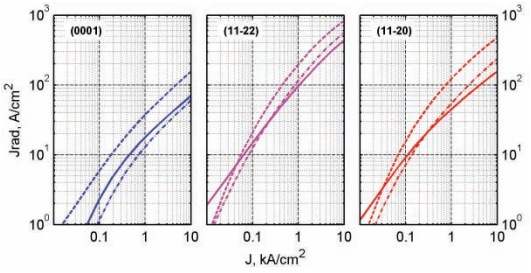

Figure 8. QW radiative currents in 3-QW diodes grown on different templates vs. diode injection.

tions notably deviate from their equilibrium values. Right panel in Figure 7 compares the resulting residual QW charges in polar and semipolar 3-QW diodes of the same design. QW charges remain quite high even in nonpolar structure with electrically uniform active region (see Figure 6). These charges can be attributed to dissimilar electron-hole transport in III-nitride heterostructures and strong carrier confinement in deep III-nitride QWs [3].

Figure 8 compares the QW optical output presented in the form of QW radiative currents for the three modeled 3-QW diodes of different polarities. Notably, the best uniformity of the radiative current distribution among all three active QWs was achieved not in the nonpolar structure with the most uniform active region but in semipolar emitter with optimum QW width.

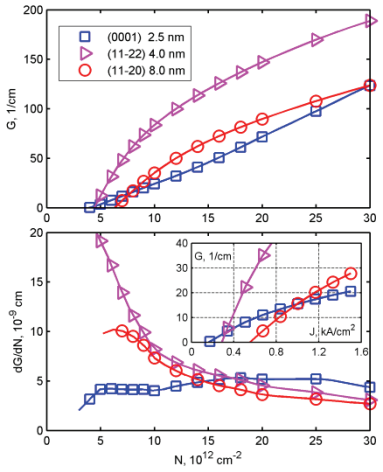

Figure 9. TE optical gain characteristics for laser diodes grown on different templates.

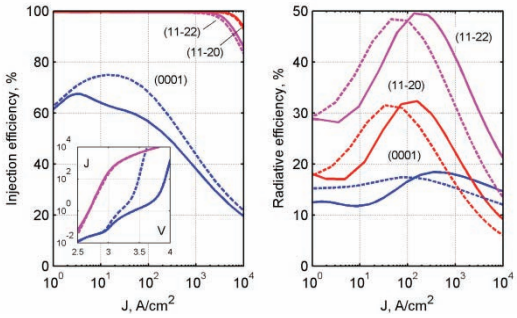

Figure 10. Efficiency characteristics of 3-QW (solid) and 1-QW (dashed) structures of different polarity.

Figures 9 compares optical gain characteristics of laser diodes. Inset in Figure 9 shows gain-current relations for modeled devices near the QW transparency injection level. The performance deterioration of nonpolar laser with widest QWs is directly related to thermal carrier redistribution between closely separated valence subbands; see Figure 1. Figure 10 compares the efficiency characteristics of corresponding light-emitting devices again illustrating the benefits of optimized semipolar structure. Dashed lines in Figure 10 indicate performance of single-QW devices. Inset compares I-V characteristics of polar and semipolar diodes.

4. References

1. M. V. Kisin, R. G. W. Brown, H. S. El-Ghoroury, in *COMSOL Conference 2009*, Boston, MA, USA. www.comsol.com/papers/6660
2. M. V. Kisin, R. G. W. Brown, H. S. El-Ghoroury, *Journal of Applied Physics*, **105**, 013112-5 (2009).
3. M. V. Kisin, H. S. El-Ghoroury, *Journal of Applied Physics*, **107**, 103106-9 (2010).
4. G. Belenky, L. Shterengas, M. V. Kisin, "GaSb based type I diode lasers. Recent development and prospects." in *Semiconductor lasers: Fundamentals and applications*, Ed. by A. Baranov and E. Tournie, Cambridge: Woodhead Publishing (2012).
5. M. V. Kisin, H. S. El-Ghoroury, in *COMSOL Conference 2010*, Boston, MA, USA. www.comsol.com/papers/7675
6. M. V. Kisin, H. S. El-Ghoroury, *Physica Status Solidi C*, **8**, 2264-2266 (2011).